



Detection of FRET efficiency in imaging systems by photo-bleaching acceptors

Chuyun Deng, Jiamin Li, Wanyun Ma*

Key Laboratory for Atomic and Molecular Nanosciences of Education Ministry, Department of Physics, Tsinghua University, Beijing 100084, China

ARTICLE INFO

Article history:

Received 8 March 2010

Received in revised form 18 May 2010

Accepted 22 May 2010

Available online 1 June 2010

Keywords:

FRET efficiency
Microscopy imaging
Photo-bleaching
Quantum dot

ABSTRACT

Fluorescence resonance energy transfer (FRET) is widely used to obtain the distance between a donor and an acceptor in biological research. However, the detection of FRET efficiencies with fluorescence microscopy imaging systems remains a great challenge due to the difficulties of transferring gray scales of the images into fluorescence intensities, and the absence of exact quantum yields of donors and acceptors. Herein, we presented a new method to detect the FRET efficiency in imaging systems by analyzing the photo-bleaching-induced changes in fluorescent intensities of quantum dots (QDs, donors) and Cy5 dyes (acceptors). Our method is different from the previous acceptor-photo-bleaching studies in imaging systems by theoretically analyzing the bleaching process, and bringing forward a new parameter which is universal for samples of the same kind. It is convenient for calculating FRET efficiencies. There is hardly any spectral crosstalk between 605QD and Cy5, thus the FRET result is more accurate than that of many other common FRET pairs. The lengths of single-stranded and double-stranded DNA fragments in solution were determined via the analysis of FRET efficiency values. This technique provides a reliable approach to study biomacromolecules in living cells through fluorescent imaging and in situ measurements.

© 2010 Elsevier B.V. All rights reserved.

1. Introduction

Fluorescence resonance energy transfer (FRET) has been used as a spectral ruler in the analysis of macromolecular interactions in the field of biomedicine. There are many different kinds of fluorescence detecting systems to measure FRET. These include fluorescence lifetime detecting systems that use a fluorescence lifetime spectrometer [1], fluorescence intensity detecting systems that use capillary and avalanche photodiodes [2] and fluorescence imaging detecting systems that use intensified CCD detectors [3]. The former two systems produce quantitative data, allowing FRET efficiency to be calculated more precisely. While the latter system is not as effective at measuring FRET efficiency, it is still invaluable for biomedical research because it allows in situ imaging and real-time detection. The two main difficulties in obtaining data on FRET efficiency using imaging systems are transferring the gray scale of the image into the fluorescence intensity which is not the same for different probes, and determining the quantum yields of donors and acceptors which change with the environment [4]. Spectral crosstalk should also be considered when calculating FRET efficiency [5]. The overlap in emission spectra of the donor and the acceptor affects the FRET signal, leading to false results. Besides, if the absorption spectra of the donor and the acceptor have crosstalk, the acceptor might be excited by the excitation source of the donor, and the FRET signal

will also be false. To obtain the correct FRET signal, the effects of spectral crosstalk should be removed from the original results.

In this study, the complexity of obtaining FRET efficiency data from fluorescence imaging detecting systems was analyzed and a new method using photo-bleaching that could eliminate the difficulties was presented. There have been many reports about obtaining FRET efficiency by photo-bleaching [6–11], however, most of them calculated the efficiency through the photo-bleaching-induced changes of fluorescence lifetimes. In our method, the photo-bleaching-induced changes of fluorescent intensities were analyzed, and a new parameter to calculate FRET efficiencies was defined, which represents the effects of experimental equipments and FRET dyes' quantum yields. This technique provides fluorescent images and in situ measurements which have unique advantages in biomedical research on cells. To simplify our work, we chose quantum dots (QDs) as the donors and Cy5 molecules as the acceptors. Our analysis was based on a FRET assembly model in which one QD and a certain number of Cy5 molecules were linked [13,14]. The FRET efficiency of one such assembly is greater than a usual FRET pair as it contains several FRET pairs. QDs have broad absorption, narrow emission and size-tunable photoluminescence spectra, thus we are able to choose an appropriate QD, 605QD, to minimize its crosstalk with Cy5 [9,15].

2. Materials and methods

Streptavidin conjugated QDs (Qdot 605ITK Streptavidin Conjugate Kit, Cat. Number: Q10001MP) were purchased from Invitrogen

* Corresponding author. Tel.: +86 1062788938x169; fax: +86 1062781598.
E-mail address: mawy@tsinghua.edu.cn (W. Ma).

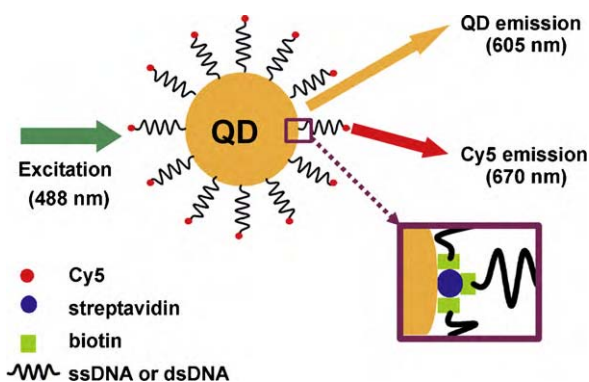


Fig. 1. Principles of FRET between QD and Cy5 in a QD-dsDNA/ssDNA complex. The streptavidins on the QD surface were bound with biotins and then Cy5-ssDNA-biotins were close to the QD. Each streptavidin bound at most three Cy5-ssDNA-biotins. With an excitation wavelength of 488 nm, the QD and Cy5s had FRET.

Co. (USA). The DNA sequence Cy5-ssDNA-biotins (Cy5-5'-AAA GGA CCA GGC GCA ACT AAA TTC A-3'-biotin) and the complementary DNA sequence (5'-TGA ATT TAG TTG CGC CTG GTC CTT T-3') were purchased from GeneCore BioTech Co. Ltd. (Shanghai, China). One streptavidin combines with three biotins at most. These combinations brought QDs and Cy5s together and FRET signals were obtained (Fig. 1). Each QD had 12–15 streptavidin molecules attached. We adjusted the concentration of QDs and Cy5-ssDNA-biotin to obtain a ratio of 1/36 (QD/Cy5) on average, that is, one QD linked with 36 Cy5 molecules. The complementary DNA sequences were used to bind Cy5-ssDNA-biotins and then Cy5-dsDNA-biotins were obtained [14]. We placed 20 μ l of this mixture (QD-ssDNA-Cy5 or QD-dsDNA-Cy5) onto a clean cover slip and placed the cover slip on our imaging stage. Our experimental system contained an inverted microscope (TE2000, Nikon, Japan), an Argon ion laser (35 LAL 415, Melles Griot, USA), a mercury lamp (Nikon, Japan) and an Intensified CCD (I-PentaMAX Gen 4, Roper Scientific, USA). Relative

spectra and a sketch of the system are shown in Fig. 2. The spectra crosstalk between 605QD and Cy5 is small enough, and there will be no false FRET signal.

3. Results and discussion

3.1. Difficulties in measuring the FRET efficiency in imaging systems

For imaging systems, the FRET efficiency (EN) is defined as [12]:

$$E_N \equiv \frac{1}{1 + ((I_d/I_a)(\phi_a/\phi_d))} \quad (1)$$

or

$$E_N \equiv 1 - \frac{I_d}{I_{dmax}} \quad (2)$$

The subscripts *a* and *d* represent acceptors and donors respectively, and *max* means the maximum value. I_d and I_a represent the fluorescent intensities of donors and acceptors when FRET occurs. Φ_d and Φ_a are the corresponding quantum yields. I_{dmax} is the fluorescent intensity of the donors when no acceptor exists, which is also the maximum value of I_d . The subscript *N* in E_N represents the number of FRET pairs, and E_1 represents the efficiency of a single FRET pair. We obtain the value of E_N from the data and then convert E_N into E_1 to calculate the FRET distance *r* using these two equations [10]:

$$E_N = \frac{NE_1}{(N-1)E_1 + 1} \quad (3)$$

$$E_1 = \frac{1}{1 + (r/r_0)^6} \quad (4)$$

According to Eq. (1), the fluorescent intensities of the donors and acceptors are needed. This is not straightforward when using imaging systems as the CCD output is a gray scale image instead of

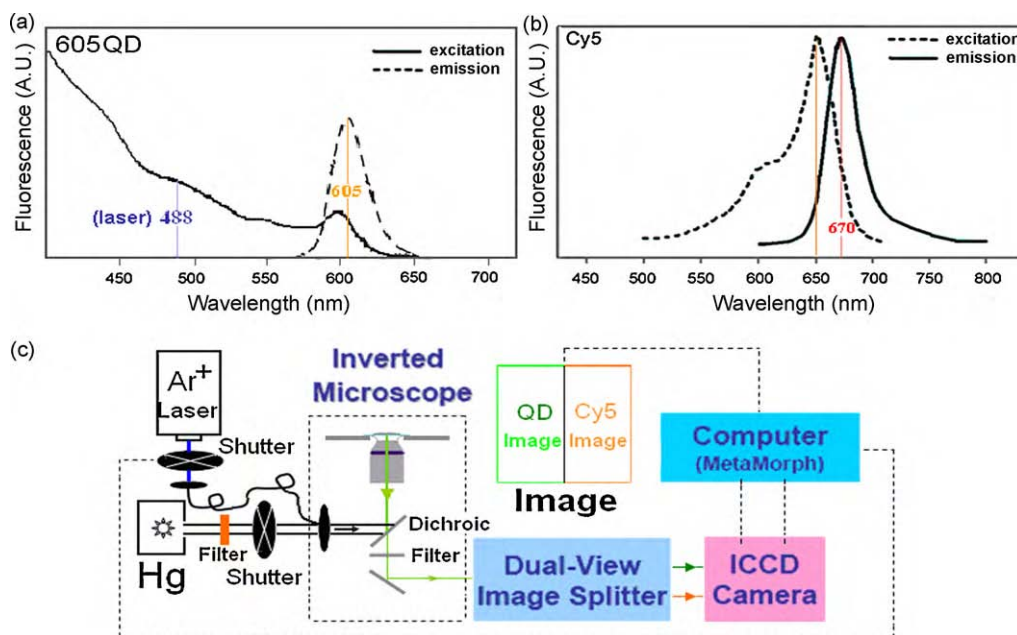


Fig. 2. The emission and excitation spectra of the acceptor (Cy5) and donors (605QD), and experimental set-up for FRET detection. (a) Emission and excitation spectra of QDs (Invitrogen, USA). The blue 488 nm line is the wavelength of the Argon ion laser, which excites QDs. The orange 605 nm line is the central wavelength of the emission spectrum. (b) Emission and excitation spectra of Cy5s. The orange 650 nm line represents the mercury lamp, which excites Cy5s. The red 670 nm line is the central wavelength of the emission spectrum. (c) The system contained two illuminators, the Argon ion laser and the mercury lamp. The mercury lamp had a broad spectrum; a proper filter was used to ensure the emission light had a wavelength of 650 nm. The shutters and the camera ICCD (intensified CCD) were controlled by the MetaMorph software. The dual-view image splitter had two signal channels, one for QDs and the other for Cy5s, so the donor and acceptor fluorescence were obtained simultaneously. (For interpretation of the references to color in this figure legend, the reader is referred to the web version of the article.)

fluorescent intensity. Usually gray scales are related to fluorescent intensities according to the following equation:

$$g = \eta \cdot I \quad (5)$$

Here g is the gray scale and I is the fluorescent intensity. η is the response of the instrument, defined as the gray scale translated from one unit fluorescent intensity. Using Eq. (5), Eq. (1) is equal to:

$$E_N = \frac{1}{1 + ((g_d/g_a)(\eta_a/\eta_d)(\phi_a/\phi_d))} \quad (6)$$

η_d could differ greatly from η_a because of different optical filters, different collection abilities and responses of the instruments. Besides, environmental changes of the fluorescence probes will change their quantum yields. Therefore η_d , η_a , ϕ_d and ϕ_a for different FRET conditions have to be determined. Eq. (6) is converted into the following two equations:

$$E_N = \frac{1}{1 + ((g_d/g_a)(1/R))} \quad (7)$$

$$R \equiv \frac{\eta_d \phi_d}{\eta_a \phi_a} \quad (8)$$

This simplifies the issue and only one parameter R needs to be determined to obtain the FRET efficiency.

On the other hand, Eqs. (2) and (5) are used to obtain the following equation:

$$E_N = 1 - \frac{g_d}{g_{dmax}} \quad (9)$$

This equation can avoid determining η_d , η_a , ϕ_d and ϕ_a . However, g_{dmax} is also difficult to measure in practice, because removing all of the acceptors in the sample after FRET measurements is a challenging operation. Besides, for in situ measurements, the visual field of the microscope must remain the same after we remove the acceptors, which means the sample cannot even be moved. If the removing step is achieved, this is still a convenient way to calculate FRET efficiency. So after investigation of the difficulties in obtaining FRET efficiency, two key points have been highlighted, R and g_{dmax} .

3.2. Obtaining R and g_{dmax} values from acceptor-photo-bleaching

During photo-bleaching, the amount of unbleached acceptors is exponentially related to the bleaching time; therefore the fluorescent intensities and efficiencies of the FRET assemblies are also connected to the bleaching time. In our method, firstly a 488 nm laser (which cannot excite Cy5) was used to excite the QDs, producing a FRET image. The illumination time was equal to the exposure time (about 50 ms). Then the illumination was switched to a mercury lamp (which cannot excite QD) to photo-bleach Cy5s during the interval of exposures (8 s). The 50 ms exposure time was neglected in calculations compared with the 8 s bleaching time. Then this procedure was repeated and a series of fluorescence images at different times were obtained, reflecting the bleaching process.

Since photo-bleaching is an exponential decaying process, taking n to be the amount of unbleached Cy5s linked to each QD and t to be the bleaching time, we have [11]:

$$n = n_0 e^{-t/t_0} \quad (10)$$

n_0 is the amount of unbleached Cy5s linked to each QD when $t=0$. t_0 is the time when n becomes n_0/e . The number of FRET pairs here is n , so the FRET efficiency is E_n . Assuming K is the energy that QDs gain from the 488 nm laser in unit time, then:

$$I_a = K \cdot E_n \cdot \phi_a \quad (11)$$

Replacing E_n with Eqs. (3) and (10), the following equation is obtained:

$$-\ln \left(\frac{K\phi_a}{I_a} - 1 \right) = -\frac{1}{t_0} t + \ln \left(\frac{E_1}{1-E_1} n_0 \right) \quad (12)$$

$K\phi_a$ is I_{amax} (when $E_n = 1$), and we define $C \equiv \ln((E_1/(1-E_1))n_0)$. Then it is equal to:

$$-\ln \left(\frac{I_{amax}}{I_a} - 1 \right) = -\frac{1}{t_0} t + C \quad (13)$$

which means:

$$-\ln \left(\frac{g_{amax}}{g_a} - 1 \right) = -\frac{1}{t_0} t + C \quad (14)$$

Besides, similar to Eq. (11),

$$I_d = K \cdot (1 - E_n) \cdot \phi_d \quad (15)$$

$I_{dmax} = K \cdot \phi_d$ while $E_n = 0$. By replacing E_n with Eqs. (9) and (10), Eq. (15) becomes:

$$\ln \left(\frac{g_{dmax}}{g_d} - 1 \right) = -\frac{1}{t_0} t + C \quad (16)$$

In addition, dividing Eq. (11) by Eq. (15), it becomes:

$$\ln \left(\frac{g_a}{g_d} \right) = -\frac{1}{t_0} t + C + \ln \left(\frac{\phi_a \eta_a}{\phi_d \eta_d} \right) \quad (17)$$

which can be expressed as:

$$\ln \left(\frac{g_a}{g_d} \right) = -\frac{1}{t_0} t + C - \ln R \quad (18)$$

By the definitions of I_{amax} and I_{dmax} , we know:

$$\frac{g_{dmax}}{g_{amax}} = \frac{\eta_d I_{dmax}}{\eta_a I_{amax}} = \frac{\phi_d \eta_d}{\phi_a \eta_a} = R \quad (19)$$

The FRET images contain the values of g_a/g_d at each time point (t). By linear fitting the values of R and g_{dmax} are determined and then E_n is calculated using the values of g_d and g_a at $t=0$.

There is a more convenient way to obtain the g_{dmax} value which does not require so many exposures. Firstly the laser was used to excite the sample and the FRET image was recorded. Secondly the mercury lamp was turned on long enough for all Cy5s to be completely photo-bleached. No FRET occurred then and the donor fluorescence was maximal. At this point, the laser was switched back to record another image. From the latter image it was possible to determine the g_{dmax} value.

Although the second method is easier to carry out, it is not appropriate when there are a large number of samples, because every sample needs to be photo-bleached, which is time-consuming. However, using the first method, once the R value has been derived, this value can be used for all similar samples and each sample only needs one shot.

4. Results

Using the first method above-described, 160 frames of fluorescent images for 159 periods was recorded. The sample was high concentration (QD concentration was 2×10^{-9} M) solution of the QD-ssDNA-Cy5 complex. High concentration samples were chosen to minimize the stochastic fluctuation of the fluorescence so that the R value was more accurate. By Eqs. (14) and (18) and linear fitting the following values were obtained: $C - \ln R = -1.00$, $C = 0.535$, so $R = 4.64$. Besides, in this step we also got $g_{amax} = 398.4$, $g_{dmax} = 1796.8$ and then $R = 4.51$ according to Eq. (19). The 2.8% difference between these two R values resulted from linear fittings. The average of these two values (4.58) was used to calculate E_n . In the first image, $g_d = 329.7$, $g_a = 364.7$, so $E = 0.84$ using Eq. (7). Fig. 3 shows the fluorescent intensities of QDs and Cy5s as functions

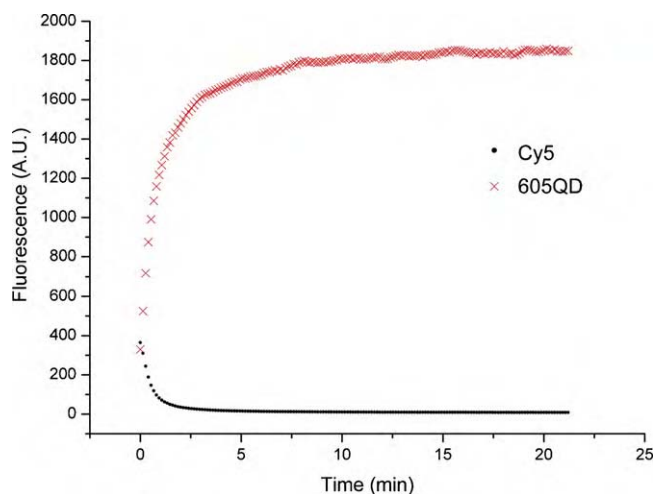


Fig. 3. The fluorescent intensities of QD and Cy5 in the bleaching. The x-coordinate was the time of illumination with the mercury lamp and the y-coordinate was the gray scale of the fluorescent signal. The curves were exponential. The fluorescent signal was the average value of a 200 pixel \times 100 pixel region, not a single pixel. This was also designed to minimize the stochastic fluctuation of the fluorescence.

of the bleaching time. The fluorescence intensity of QDs increased with the time, while the fluorescence intensity of Cy5s decreased with the time. This is attributed to the illumination-induced photo-bleaching of Cy5s, which leads to less acceptor and consequently the decrease of FRET efficiency.

The first and the last ones of the 160 frames were picked out as the beginning and ending of the photo-bleaching. Using the second method described above, the following values were obtained: $g_d = 329.7$, $g_{dmax} = 1796.8$, then $E = 0.82$ using Eq. (9). This efficiency (0.82) is very close to the former (0.84) obtained from the first method. Besides, it is difficult in practice to bleach all of the acceptors completely, and extending the bleaching time will bring a more accurate result.

To demonstrate the reliability of our theory, we analyzed some samples of ssDNA fragments and the corresponding dsDNA fragments in solution. The FRET efficiencies were calculated and compared using the R value obtained. Fig. 4 shows the fluorescent images of QD-ssDNA-Cy5 assemblies and QD-dsDNA-Cy5 assemblies. In average, with $R = 4.58$, for ssDNA, $E_{36} = 0.79 \pm 0.04$, and for dsDNA, $E'_{36} = 0.56 \pm 0.03$. From Eq. (3), $E_1 = 0.095 \pm 0.020$ and $E'_1 = 0.034 \pm 0.004$. Using Eq. (4) and $r_0 = 6.94$ nm [2], $r = 10.11 \pm 0.40$ nm

and $r' = 12.11 \pm 0.25$ nm for ssDNA and dsDNA respectively were obtained. We may conclude that dsDNA was longer than its corresponding ssDNA in solution, which was consistent with previous study. The contour length of the 25-mer dsDNA was much smaller than its persistence length (~ 50 nm), making it relatively stiff in solution, while the contour length of the 25-mer ssDNA was much larger than its persistence length (~ 1.6 nm), thus the ssDNA was more flexible and could form a random coiled conformation, which brought the probes spatially closer and led to shorter FRET distance [14].

5. Conclusion

In this study, a convenient method to obtain FRET efficiency and determine the FRET distance in situ with imaging systems was provided based on the photo-bleaching of acceptor molecules. This method would have important application in studying the interaction between biomacromolecules in living cells, such as DNA, RNA and protein, which needs imaging and in situ measurements.

Acknowledgments

The authors thank Dr. Chunyang Zhang for helpful advice. This work was supported by the National Nature Science Foundation of China (grants 90919012 and 10874099) and the Doctoral Program Research Fund of Chinese Ministry of Education (grant 20090002110065).

References

- [1] R.R. Duncan, *Biochem. Soc. Trans.* 34 (2006) 679–682.
- [2] C.Y. Zhang, H.C. Yeh, M.T. Kuroki, T.H. Wang, *Nat. Mater.* 4 (2005) 826–831.
- [3] D.Y. Lin, W.Y. Ma, S.J. Duan, Y. Zhang, L.Y. Du, *Apoptosis* 11 (2006) 1289–1298.
- [4] I. Tatischeff, R. Klein, *Photochem. Photobiol.* 22 (1975) 221–229.
- [5] H. Wallrabe, A. Periasamy, *Curr. Opin. Biotechnol.* 16 (2005) 19–27.
- [6] Y.P. Ho, H.H. Chen, K.W. Leong, T.H. Wang, *J. Control. Rel.* 116 (2006) 83–89.
- [7] A. Hillisch, M. Lorenz, S. Diekmann, *Curr. Opin. Struct. Biol.* 11 (2001) 201–207.
- [8] T. Zal, N.R.J. Gascoigne, *Biophys. J.* 86 (2004) 3923–3939.
- [9] T. Jamieson, R. Bakhshi, D. Petrova, R. Pocock, M. Imani, A.M. Seifalian, *Biomaterials* 28 (2007) 4717–4732.
- [10] A.R. Clapp, I.L. Medintz, J.M. Mauro, B.R. Fisher, M.G. Bawendi, H. Mattoussi, *J. Am. Chem. Soc.* 126 (2004) 301–310.
- [11] A.H.A. Clayton, N. Klonis, S.H. Cody, E.C. Nice, *Eur. Biophys. J.* 34 (2005) 82–90.
- [12] G.W. Gordon, G. Berry, X.H. Liang, B. Levine, B. Herman, *Biophys. J.* 74 (1998) 2702–2713.
- [13] D.M. Willard, L.L. Carillo, J. Jung, A.V. Orden, *Nano Lett.* 1 (2001) 469–474.
- [14] C.Y. Zhang, L.W. Johnson, *Anal. Chem.* 78 (2006) 5532–5537.
- [15] H.E. Grecco, K.A. Lidke, R. Heintzmann, D.S. Lidke, C. Spagnuolo, O.E. Martinez, E.A. Jares-Erijman, T.M. Jovin, *Microsc. Res. Techn.* 65 (2004) 169–179.

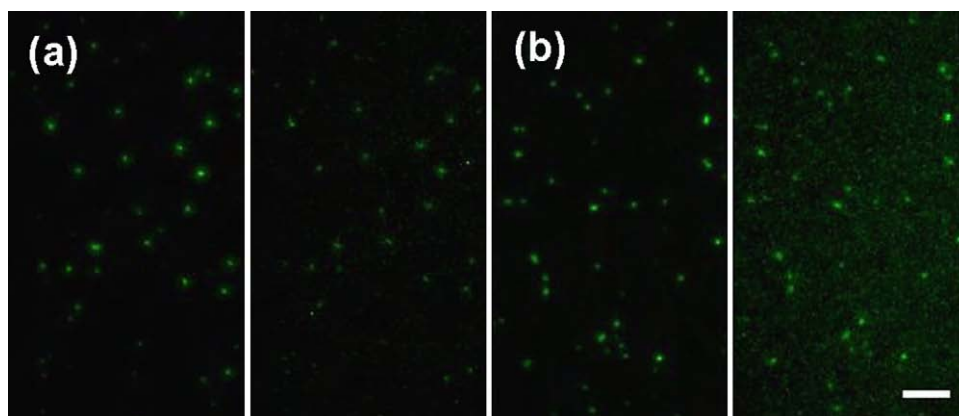


Fig. 4. The dual-channel fluorescent images of QD-ssDNA-Cy5 assemblies and QD-dsDNA-Cy5 assemblies. (a) QD-ssDNA-Cy5 assemblies; (b) QD-dsDNA-Cy5 assemblies. For each image, the left channel (605 nm) was for 605QD, and the right channel (670 nm) was for Cy5. The bar was 10 μ m.